Materials Research. 2016; 19(4): 942-953
DOI: http://dx.doi.org/10.1590/1980-5373-MR-2016-0157

Assessment of the Ti-Rich Corner of the Ti-Si Phase Diagram: The Recent Dispute About the Eutectoid Reaction

Marina Fiore[a], Flavio Beneduce Neto[a], Cesar Roberto de Farias Azevedo[a]*

[a]Department of Metallurgical and Materials Engineering, Escola Politécnica, Universidade de São Paulo – USP, Av. Professor Mello Moraes, 2463, 05508-030, São Paulo, SP, Brazil

Received: February 24, 2016; Revised: May 3, 2016; Accepted: June 5, 2016

The thermodynamic optimization of Ti-Si-X systems requires that their respective binary systems are constantly updated. The Ti-Si system has been experimentally investigated since the 1950s and these critical experimental data can be employed to calculate the Ti-Si phase diagram using thermodynamic modeling. The most recent assessment of the Ti-Si system was performed in 1998, showing the presence of stoichiometric Ti_3Si as stable phase. In the light of the dispute over the stability of Ti_3Si phase in the eutectoid reaction of the Ti-Si and Ti-X-Si systems, the present work assessed the Ti-rich corner of the "stable" (featuring Ti_3Si phase) and "metastable" (featuring Ti_5Si_3 phase) Ti-Si phase diagrams. The phase boundaries, the values of the error of the least-square method of the optimization procedure and the relative standard deviation of the calculated variables of the assessed diagrams; and previous investigations were discussed in order to inspire further experimental work on the eutectoid reaction of the Ti-Si phase diagram.

Keywords: *Ti-Si phase diagram, Ti-rich corner, thermodynamic modeling, sublattice model, eutectoid reaction*

1. Introduction

There is a continuous technological interest in the Ti-Si system, which is promoted by the beneficial effect of Si addition on the oxidation and creep resistance (via solid solution and precipitation hardening) of Ti-X-Si alloys[1]. The earliest Ti-Si phase diagram was thoroughly investigated in 1952 by Hansen et al.[2], which studied more than fifty Ti-Si binary alloys. The absence of interstitial contamination during the casting of these alloys was verified by hardness measurements of control samples of pure Ti. The microstructure was characterized by metallography and X-ray diffraction, while the transition temperatures were determined by incipient melting point studies and thermal analysis. Their results showed that non-stoichiometric Ti_5Si_3 phase existed over a composition range from 38 to 40at% Si. The phase diagram indicated in the Ti-rich corner the presences of a eutectic reaction at 1606K, L $\rightarrow$ Ti(β) + Ti_5Si_3, and a eutectoid reaction at 1133K, Ti(β) $\rightarrow$ Ti(α) + Ti_5Si_3. The presence of this eutectoid reaction was confirmed by the investigation of seven Ti-Si alloys containing up to 2% Si, which were heat-treated between 1023K and 1373K for times of respectively 170 and 31 hours. In 1954 Sutcliffe[3,4] investigated the Ti-rich corner of the Ti-Si system using isothermal heat-treatments of homogenized samples at temperatures between 923K and 1373K for 720 to 72 hours, respectively. Control samples and hardness measurements were also used to ensure that the interstitial content (O and N) in the alloys was below 0.05wt%. They confirmed the presence of a eutectoid reaction at 1129K, Ti(β) $\rightarrow$ Ti(α) + Ti_5Si_3, but presenting smaller Si solubility (~40%) in the Ti(β) phase than previous result[2].

In 1970, Svechnikov et al.[5] proposed a new experimental version of the Ti-Si phase diagram with the presence of a stoichiometric Ti_3Si phase (tetragonal, Ti_3P crystal structure). They studied thirty Ti-Si alloys, which were analyzed by differential thermal analysis (DTA), metallography and X-ray diffraction. The experimental procedure did not explicitly describe the use of control samples to ensure the lack of interstitial contamination in the alloys. The stoichiometric Ti_3Si phase was identified in Ti-rich samples after heat-treatment at 1273K for 115 hours and 1493K for 120 hours. The Ti-rich corner of the experimental phase diagram showed unusual phase boundaries, featuring, for instance, the presence of Ti_3Si phase until the eutectic reaction, L $\rightarrow$ Ti(β) + Ti_5Si_3, and the presence of atypical boundaries at 1443K, dividing into two regions the [Ti(β)+Ti_3Si] and [Ti_3Si+Ti_5Si_3] phase fields, respectively. Finally they suggested the presence of two new reactions in the Ti-rich corner: a peritectoid reaction at 1444K, Ti(β) + Ti_5Si_3 $\rightarrow$ Ti_3Si, and a eutectoid reaction at 1133K, Ti(β) $\rightarrow$ Ti(α) + Ti_3Si.

In 1977 and 1978 Aaronson et al.[6,7] investigated the eutectoid reaction of the Ti-rich corner of the Ti-Si system, using continuous cooling experiments, microstructural characterization and microanalysis. Isothermal heat-treatments of homogenized samples were carried out at 1023K for 24 and 120 hours. Chemical analysis of interstitials (C, O, N, and H) after the homogenization heat-treatment indicated that their alloys contained approximately 0.04wt%C, 250 to 350 ppm of O_2, 65 ppm of H_2 and 200 ppm of N_2. None of the previous works[2-5] actually used chemical analysis to check the amount of interstitials in the investigated alloys. The authors did not observe any precipitation of Ti_3Si phase, as proposed by Svechnikov et al.[5], confirming, instead, the presence of a eutectoid reaction at 1148K, Ti(β) $\rightarrow$ Ti(α) + Ti_5Si_3, as observed by previous investigations[2-4]. Their results also featured higher Si solubility in the Ti(β) phase

* e-mail: c.azevedo@usp.br

and lower Si solubility in the Ti(α) than previous works[3,4]. Plitcha and Aaronson[6,7] concluded that the differences between their version of the eutectoid reaction of the Ti-Si system and previous results could be due to the higher impurity contents in the alloys previously investigated.

The first thermodynamic assessment of the Ti-Si phase diagram was performed by Kaufmann[8] in 1976. This assessment was based on the experimental results of Hansen et al.[2], but considering the Ti_5Si_3 phase as a stoichiometric intermetallic. Kaufmann[8] did not provide any information about the optimization procedure and his calculated diagram was a simplistic version of previous experimental phase diagrams[2-4]. Murray[9] in 1987 assessed the Ti-Si system and the assessed phase diagram[9] was in fair agreement with the experimental results of Svechnikov et al.[5], showing the presences of a peritectoid reaction at 1443K, Ti(β) + Ti_5Si_3 → Ti_3Si, and a eutectoid reaction at 1138K, Ti(β) → Ti(α) + Ti_3Si. Additionally, the phase diagram featured the presence of non-stoichiometric Ti_5Si_3 phase. In 1989 Vahlas et al.[10] assessed the Ti-Si system and their calculated diagram showed a much simpler version of previous assessment[9], featuring the presence of Ti_5Si_3 phase as a stoichiometric intermetallic.

In 1996 Seifert et al.[11] employed software using Gaussian least square optimization method for the determination of the adjustable optimizing variables of the thermodynamic functions to assess the Ti-Si system. They tested two different thermodynamic descriptions for the liquid phase: the regular solution model using the Redlich-Kister formalism; and the partially ionic liquid model. Their calculated phase diagram was in fair agreement with the calculated diagram proposed by Murray[9] and the experimental diagram proposed by Svechnikov et al.[5], indicating in the Ti-rich corner of phase diagram the presences of a peritectoid reaction at 1443K, Ti(β) + Ti_5Si_3 → Ti_3Si, and a eutectoid reaction at 1138K, Ti(β) → Ti(α) + Ti_3Si. The authors did not use the experimental results of Aaronson and Plitcha[6,7] for the eutectoid reaction, which did not confirm the presence of Ti_3Si phase. Additionally, they did not find in the literature any experimental data for the Si solubility in the Ti(α) and Ti(β) phases of the eutectoid reaction, Ti(β) → Ti(α) + Ti_3Si, so they assumed that the Si solubility in these phases was equal to previous experimental results[2] for the "metastable" eutectoid reaction, Ti(β) → Ti(α) + Ti_5Si_3.

Concerning the dispute over the stability of the Ti_3Si phase in Ti-Si and Ti-Al-Si alloys, Azevedo et al.[1,12-14] investigated in 1996 the Ti-rich corner of the Ti-Al-Si system using control samples (hardness measurements), TEM, EDS and electron diffraction. Their results did not show the presence of Ti_3Si phase after isothermal heat-treatment at 973K for 36 days, but the presence of a ternary non-stoichiometric Ti_5Si_3 phase. In 1997, Bulanova et al.[15] also could not identify the presence of Ti_3Si phase in Ti-13.5Si alloy after heat-treatments at 1323K for 45 hours and 1023K for 58 hours by XRD and microanalysis. The presence of Ti_3Si phase in a Ti-13.5Si alloy was observed by Ramos et al.[16] in 2006 after isothermal heat-treatments at 1273K and 1373K for 90 hours by SEM-EDS analysis. In 2010 Costa et al.[17] observed the presence of Ti_3Si phase in Ti-13Si and Ti-20Si alloys after isothermal heat-treatment at 1273K for various times by XRD. In 2014 Li et al.[18] observed the presence of Ti_3Si phase in a Ti-15Si-5Al alloy after isothermal heat-treatment for 45 days at 973K using microanalysis coupled with XRD. Finally, in 2014 Kozlov et al.[19] observed the presence of Ti_3Si phase in Ti-Si and Ti-Ge-Si alloys after isothermal treatments of at 943K for 720 hours by XRD.

Colinet and Tedenac[20] studied in 2010 the structural stability of intermetallic phases in the Ti-Si system by ab-initio calculations. A statistical model was used to obtain the enthalpy for the formation of the intermetallic phases. The predicted ground-state structures were consistent with those known to be stable at low temperature, except for the Ti_3Si phase with Ti_3P (tP32) structure, whose enthalpy of formation at 0K (-47.11 kJ/mol of atoms) was slightly above the ground-state line, indicating that the question of stability of the Ti_3Si phase shown by previous experimental[5] and calculated[9,11] Ti-Si phase diagrams was in fact "controversial". More recently, Poletaev et al.[21] indicated that Ti_5Si_3 phase was actually more stable than Ti_3Si phase at 0 K by ab initio calculations. They also confirmed the presence of Ti(α) and Ti_5Si_3 phases by electron diffraction and microanalysis after the heat-treatment of a Ti-0.7Si alloy at 873K for 10 hours.

In the light of the dispute over the stability of Ti_3Si phase in Ti-X-Si engineering alloys[2-21], the present work will calculate and compare the Ti-rich corner of the "stable" and "metastable" Ti-Si phase diagrams, by assuming that Ti_3Si is the stable phase in the eutectoid reaction, Ti(β) → Ti(α)+ Ti_3Si. These results will be discussed in order to inspire further experimental work on critical regions of the Ti-Si phase diagram[11].

2. Methodology

The present work calculated the stable and metastable Ti-Si phase diagrams (assuming that Ti_3Si is the stable phase in the eutectoid reaction, Ti(β) → Ti(α)+ Ti_3Si), using Thermocalc software and COST 507 (Thermochemical Database for Light Metal Alloys)[22], whose principle objective was to provide a computerized thermodynamic database to permit the calculation of multicomponent phase equilibria for light alloys based on aluminum, magnesium and titanium to aid in the development of commercial light alloys under the organization of the European Cooperation in Science and Technology.

The liquid phase; and Ti(α) and Ti(β) solid solution phases were described using Equations 1 to 5 (see Annex 1). The Gibbs free energy of reference (G^{ref}) describes the mechanical mixing of pure elements (see equation 2), while the Gibbs free energy of the ideal solution (G^{id}) was described by equation 3 and the excess Gibbs free energy (G^{ex}) was described using the Redlich-Kister polynomial (see Equations 4 and 5)[23]. The Gibbs energy for the formation of stoichiometric Ti_3Si phase was described using the Kopp-Neumann rule[23], see Equation 6 and a more detailed description is given in Annex 1.

$$G_{phase} = G^{ref} + G^{id} + G^{ex} \qquad (1)$$

$$G^{ref} = x_{Si} \cdot G^{ref}_{Si} + x_{Ti} \cdot G^{ref}_{Ti} \qquad (2)$$

Where: $G_i^{ref} = G_i^{SER}$ *and* x_{Si} *and* x_{Ti} *are the molar fraction of the elements. The superscript 'SER' refers to the Standard Element Reference state.*

$$G^{id} = R \cdot T \cdot [x_{Si} \cdot \ln x_{Si} + x_{Ti} \cdot \ln x_{Ti}] \quad (3)$$

$$G^{exc} = x_{Si} \cdot x_{Ti} \cdot L_{phase} \quad (4)$$

Where: L^i_{phase} *is the Ti-Si interaction parameter.*

$$L_{phase} = L^0_{phase} + L^1_{phase}(x_{Si} - x_{Ti}) + ... + L^v_{phase}(x_{Si} - x_{Ti})^v \quad (5)$$

Where: $L^v_{phase} = a + bT + ...$

$$G^{form}_{Ti_3Si} - x_{Ti} \cdot G^{SER}_{Ti} - x_{Si} \cdot G^{SER}_{Si} = a + b \cdot T + c \cdot T \cdot \ln(T) \quad (6)$$

The non-stoichiometric Ti_5Si_3 phase was described by the Compound Energy Formalism[23], using a three sublattices configuration, $(Ti,Si)_2(Si,Ti)_3(Ti)_3$ (see Equations 7 to 10) as suggested previously[11]. These authors[11] described the Ti_5Si_3 phase as a non-stoichiometric compound containing three sublattices to represent its $D8_8$ crystal structure - 4 atoms of Ti in the position 4(d), 6 atoms of Ti in the position 6(g) and 6 atoms of Si in the position 6(g): $(Ti,Si)_2$:$(Si,Ti)_3$:$(Ti)_3$. Colinet and Tedenac[20], for instance, used a four sublattices configuration to describe the Ti_5Si_3 phase in order to account for the $D8_8$ structure and for the possibility of inserting Si atoms in the 2b Wyckoff positions of $P6_3/mcm$ space group. The use of a four sublattices $((Si,Ti)^{\alpha}(Ti)^{b1}(Ti)^{b2}(V,Si)^{\gamma})$ to describe the Ti_5Si_3 phase[20] was not considered in the present work as it might significantly increase the number of excess terms to be calculated during the optimization procedure of higher order systems.

The parameters used of the thermodynamic description of the Ti_5Si_3 and Ti_3Si phases in the present work are listed in Table 1 and more detailed thermodynamic description of the phases is given in Annex1. Note that the value for the Gibbs energy for the formation of Ti phase with $D8_8$ crystal structure was not calculated in the present work, so the value listed for this parameter was directly copied from the COST 507 thermochemical database[22].

$$G^{Ti5Si3} = {}^{form}G^{Ti5Si3} + {}^{id}G^{Ti5Si3} + {}^{ex}G^{Ti5Si3} \quad (7)$$

$${}^{form}G^{Ti_5Si_3} = y'_{Ti} \cdot y''_{Ti} \cdot G^{ref}_{Ti:Ti:Ti} + y'_{Ti} \cdot y''_{Si} \cdot G^{ref}_{Ti:Si:Ti} + y'_{Si} \cdot y''_{Si} \cdot G^{ref}_{Si:Si:Ti} + y'_{Si} \cdot y''_{Ti} \cdot G^{ref}_{Si:Ti:Ti} \quad (8)$$

$${}^{id}G^{Ti_5Si_3} = R \cdot T \cdot \begin{pmatrix} 2 \cdot [y'_{Ti} \cdot \ln(y'_{Ti}) + y'_{Si} \cdot \ln(y'_{Si})] + \\ 3 \cdot [y''_{Ti} \cdot \ln(y''_{Ti}) + y''_{Si} \cdot \ln(y''_{Si})] \end{pmatrix} \quad (9)$$

$${}^{ex}G^{Ti_5Si_3} = y'_{Ti} \cdot y'_{Si} \cdot (y''_{Ti} \cdot {}^0L^{Ti_5Si_3}_{Ti,Si:Ti:Ti} + y''_{Si} \cdot {}^0L^{Ti_5Si_3}_{Ti,Si:Si:Ti}) + y''_{Ti} \cdot y''_{Si} \cdot (y'_{Ti} \cdot {}^0L^{Ti_5Si_3}_{Ti:Si,Ti:Ti} + y'_{Si} \cdot {}^0L^{Ti_5Si_3}_{Si:Si,Ti:Ti}) \quad (10)$$

Where: $y^{(n)}_j$ *is the site fraction of the element (j) in the sublattice (n).*

The Parrot module of the Thermocalc software was used for the determination of the optimizing variables of the thermodynamic functions describing Ti_3Si and Ti_5Si_3 phases, using selected experimental data, including the invariant reactions shown in Table 2. The experimental data for the eutectoid temperature and the Si solubility in the Ti(α) and Ti(β) phases in the "stable" eutectoid reaction, Ti(β) → Ti(α) + Ti_3Si, was estimated based on previous experimental results[2] for the "metastable" eutectoid reaction, Ti(β) → Ti(α) + Ti_5Si_3, using adjustment factors for correcting the values of the eutectoid temperature and the Si solubility in the Ti(α) and Ti(β) phases. These factors were based in the changes of the eutectoid temperature and C solubility of the Fe(γ) and Fe(α) phases in the Fe-C phase diagram for the stable, Fe(γ,2.97%C) → Fe(α,0.096%C%) + C(graphite) at 740ºC, and metastable, Fe(γ,3.46%C) → Fe(α,0.104%) + Fe_3C at 727ºC, eutectoid reactions[24]. The absolute error in the experimental values was assumed to be equal to 10K for the incongruent temperatures; and between 0.02 and 0.001 for the Si solubility, (atomic fraction of Si). Finally, the same weight was attributed to all the experimental data used in the present assessment. Table 3 shows the values for the enthalpy for the formation of intermetallic phases used in the present investigation[11,20,25-30]. Colinet and Tedenac[20], for instance, obtained the values of the enthalpy for the formation of the intermetallic phases at 0K via ab-initio calculations and statistical modelling.

The missing variables of the Ti_5Si_3 phase (see Table 1) were initially calculated during the optimization procedure of the metastable Ti-Si phase diagram (by suspending the presence of the Ti_3Si phase). These calculated values were fixed for the calculation of the missing variables of the Ti_3Si phase during the optimization of the stable Ti-Si phase diagram.

3. Results and discussion

The calculated values of the variables used for the description of Ti_3Si and Ti_5Si_3 phases of the present work were compared with the values calculated by Seifert et al.[11], using the regular model for describing the liquid phase. This comparison showed the same order of magnitude for most calculated variables (see Table 4). The main differences were observed for V31 (used for the description of the Gibbs energy for the formation of hypothetic Ti_6Si_2 phase); and V1 and V2 (used for the description of the Gibbs energy for the formation Ti_3Si phase) variables. Additionally, the present investigation used three variables, instead of two variables, to describe the Ti_3Si phase. According to Thermo-Calc data optimization user guide version 2015a[31], values of Vi1-type variables around 10^5 might indicate that either there were too many variables describing the Ti_5Si_3 and Ti_3Si phases or that the user did not set "proper weights" on the experimental data during the optimization procedure. Additionally, the same source[31] stated that Vi2-type variables should not present values in the order of 10 or more, as this may lead to either the presence of "inverted miscibility gaps" or the re-stabilization of a phase at high temperature. In the present assessment just one out of six Vi1- variables presented value below 10^5 (see Table 4); while half of the Vi2-type variables presented values below the order of 10. Finally, the optimization procedures for the calculation of the stable and metastable phase diagrams showed values for the reduced sum of squares approximately equal to 10, which are above the recommended value of one[31]. These results suggest that

Table 1: Parameters and variables used for the thermodynamic description of the Ti_5Si_3 and Ti_3Si phases. Vi1 in (J.(mol of atoms)$^{-1}$); Vi2 and Vi3 in (J.(mol of atoms)$^{-1}$).K^{-1}).

Thermodynamic description	Parameters	Optimizing variables
Gibbs energy for the formation of hypothetic Ti_3Si_5 (D88 crystal structure)	${}^0G^{Ti_5Si_3}_{Si:Si:Ti} - [3 \cdot G^{hcp}_{Ti}(T) + 5 \cdot G^{diamond}_{Si}(T)]$	*V11 + V12.T*
Gibbs energy for the formation of Ti_5Si_3 ($D8_8$ crystal structure)	${}^0G^{Ti_5Si_3}_{Ti:Si:Ti} - [5 \cdot G^{hcp}_{Ti}(T) + 3 \cdot G^{diamond}_{Si}(T)]$	*V21 + V22.T*
Gibbs energy for the formation of hypothetic Ti ($D8_8$ crystal structure)[22]	${}^0G^{Ti_5Si_3}_{Ti:Ti:Ti} - [8 \cdot G^{hcp}_{Ti}(T)]$	*(40000 + 20.T)*
Gibbs energy for the formation of hypothetic Ti_6Si_2 ($D8_8$ crystal structure)	${}^0G^{Ti_5Si_3}_{Si:Ti:Ti} - [6 \cdot G^{hcp}_{Ti}(T) + 2 \cdot G^{diamond}_{Si}(T)]$	*V31+ V32.T*
Excess Gibbs energy for the interaction Ti: Si,Ti:Ti	${}^0L^{Ti_5Si_3}_{Ti:Si,Ti:Ti}$	*V41 + V42.T**
Excess Gibbs energy for the interaction Si: Si,Ti:Ti	${}^0L^{Ti_5Si_3}_{Si:Si,Ti:Ti}$	*V41 + V42.T**
Excess Gibbs energy for the interaction Ti,Si:Ti:Ti	${}^0L^{Ti_5Si_3}_{Ti,Si:Ti:Ti}$	*V51 + V52.T**
Excess Gibbs energy for the interaction Ti,Si:Si:Ti	${}^0L^{Ti_5Si_3}_{Ti,Si:Si:Ti}$	*V51 + V52.T**
Gibbs energy for the formation of stoichiometric Ti_3Si	${}^0G^{Ti_3Si}_{Ti:Si} - [3 \cdot G^{hcp}_{Ti}(T) + G^{diamond}_{Si}(T)]$	*V1 + V2.T +V3.T.lnT*

$*{}^0L^{Ti_5Si_3}_{Ti,Si:Ti:Ti} = {}^0L^{Ti_5Si_3}_{Ti,Si:Si:Ti} and\ {}^0L^{Ti_5Si_3}_{Ti:Si,Ti:Ti} = {}^0L^{Ti_5}_{Si:Si,Ti:Ti}$ [11,23]

the further experimental data and better modeling of the liquid phase are needed to improve the assessment of the present Ti-Si phase diagram. Seifert et al.[11], for instance, also used the partially ionic liquid model to describe the liquid phase and their results apparently showed a better fit between the calculated and the experimental results for most of the reactions involving the liquid phase when compared to their results using the regular solution model to describe the liquid phase.

Table 5 compares the experimental and the calculated equilibriums obtained in the present assessment for the stable and metastable Ti-Si phase diagrams. Five out of 37 calculated values presented a relative deviation above 5% when compared to the experimental values. Most of these deviations were originated in the equilibriums involving the liquid phase, such as the L→ β+ Ti_5Si_3 reaction, which presented a deviation of 20% for the value of the Si solubility in Ti(β) phase and a value of 9.5% for the Si solubility in the liquid phase. These deviations involving the liquid phase might be decreased by using more complex models for the thermodynamic description of the liquid phase, such as the ionic two-sublattice liquid model; the associate liquid model; or the quasi-chemical model[23]. The remaining deviation values above 5% were found in the stable diagram, more specifically in following reactions:

- the peritectoid reaction, β +Ti_5Si_3→Ti_3Si, which presented a deviation of 30% for the Si solubility in the Ti(β) phase;
- the eutectoid reaction, β→α+Ti_3Si, which presented a deviation of 7.5% for the Si solubility in the Ti(α) phase.

These results indicate that there is a vital need for obtaining more reliable experimental data in these critical regions. For instance, the experimental results of the peritectoid reaction are still based on the work of Svechnikov et al.[5] made in the 70´s. Additionally, the experimental data for the stable eutectoid reaction, β→α+Ti_3Si, and their respective Ti(α) and Ti(β) solvus lines were not found in the literature[5,11].

The calculated values of the enthalpy and the entropy of the formation of the intermetallic phases in the Ti-Si system are shown in Table 6 and Figures 1-a and 1-b. The calculated values of enthalpy are in fair agreement with the values found in the literature[11,20,25-30], especially for the intermetallics phases in the Ti-rich corner, such as the Ti_5Si_3 and Ti_3Si phases. Figure 1-a shows the enthalpies of the formation of the Si-Ti compounds, comparing the present and previous results[11,20,25-30]. This comparison confirmed a better agreement of the enthalpy values in the Ti-rich corner (Ti_3Si and Ti_5Si_3 phases). According to Kematick and Meyers[28], the highest melting point for the compound in a system usually coincides which the position of the most negative value of the enthalpy (such as the Ti_5Si_4 phase, in according with Figure 1-a and Table 6). Figure 2-a, however, indicates that the highest melting point for the compound in the calculated Ti-Si diagram is found for the Ti_5Si_3 phase. Figure 1-b shows the entropy of the formation of the Si-Ti compounds, featuring a maximum value of entropy for the Ti_3Si phase, but this type of entropy curve could not be found in the literature in order to be compared with the present results.

Figure 2-a shows a general view of the calculated stable Ti-Si phase diagram, indicating that the positions of the phase boundaries are in fair agreement with previous assessment[11]. Figure 2-b shows a detail of the Ti-rich corner of the stable Ti-Si phase diagram near the eutectoid reaction, β→α+Ti_3Si, indicating that there is a lack of experimental data concerning the positions of the Ti(α) and Ti(β) solvus lines. Figure 2-c compares the present assessment with the calculated Ti-Si phase diagram using the COST 507 database[22] in the region of the eutectoid reaction. The present assessment shows lower values for the Si solubility in the Ti(α) and Ti(β) phases, especially for the Ti(β) phase.

Table 2: Experimental data for the invariant reactions used for the calculation of the "stable" and "metastable" Ti-Si phase diagrams (X^{phase}_{Si}: *atomic fraction of Si in the phase*).

Reaction	Experimental values		References
$L=Ti_5Si_3$	T(K)	2403	[2-5]
	X_{Si}	0.375	[2-5]
$L=TiSi_2$	T(K)	1773	[2-5]
	X_{Si}	0.667	[2-5]
$L=\beta + Ti_5Si_3$	T(K)	1613	[2-5]
	X^{L}_{Si}	0.137	[2,5]
	X^{β}_{Si}	0.05**	[11]
	$X^{Ti_5Si_3}_{Si}$	0.36**	[11]
$L=TiSi_2 + Si$	T(K)	1603	[2-5]
	X^{L}_{Si}	0.86	[2-5]
	$X^{TiSi_2}_{Si}$	0.667	[2-5]
	X^{Si}_{Si}	1	[2-5]
$L=TiSi_2 + TiSi$	T(K)	1743	[2-5]
	X^{L}_{Si}	0.641	[2-5]
	X^{TiSi}_{Si}	0.5	[2-5]
	$X^{TiSi_2}_{Si}$	0.667	[2-5]
$L + Ti_5Si_3=Ti_5Si_4$	T(K)	2193	[2-5]
	X^{L}_{Si}	0.48	[2-5]
	$X^{Ti_5Si_3}_{Si}$	0.398**	[11]
	$X^{Ti_5Si_4}_{Si}$	0.444	[2-5]
$L + Ti_5Si_4=TiSi$	T(K)	1843	[2-5]
	X^{L}_{Si}	0.60	[2-5]
	$X^{Ti_5Si_4}_{Si}$	0.444	[2-5]
	X^{TiSi}_{Si}	0.5	[2-5]
$\beta + Ti_5Si_3=Ti_3Si$	T(K)	1443	[5, 11]
	X^{β}_{Si}	0.04	[5, 11]
	$X^{Ti_5Si_3}_{Si}$	0.36**	[11]
	$X^{Ti_3Si}_{Si}$	0.25	[5, 11]
$\beta=\alpha + Ti_3Si$	T(K)	1149*	[2, 5, 11, 24]
	X^{β}_{Si}	0.009*	[2, 5, 11, 24]
	X^{α}_{Si}	0.004*	[2, 5, 11, 24]
	$X^{Ti_3Si}_{Si}$	0.25	[5, 11]
$\beta=\alpha + Ti_5Si_3$	T(K)	1130	[2-4, 6-7]
	X^{β}_{Si}	0.011	[2-4, 6-7]
	X^{α}_{Si}	0.005	[2-4, 6-7]
	$X^{Ti_5Si_3}_{Si}$	0.375	[2-4, 6-7]

*: extrapolated values; **: read from the calculated phase diagram

Table 3: Enthalpy for the formation of the intermetallic phases of the Ti-Si system at 298 K (kJ/mol).

Ti_3Si	Ti_5Si_3	Ti_5Si_4	TiSi	$TiSi_2$	Type	Reference
-50.0	- 72.67	-79.0	-77.76	-57.036	Calculated by optimization	[11]
- 47.11	- 72.53	-74.63	- 72.23	-49.87	Ab-initio, T= 0K	[20]
-	- 72.52	-	-	-	Experimental	[25]
-	-	-	-	- 56.97	Experimental	[26]
-	- 72.42	-	-	-	Experimental	[27]
-	- 78.1	- 75.9	-71.5	- 53.5	Experimental	[28]
-	- 73.8	- 78.5	- 72.6	-	Experimental	[29]
- 49	-	-	-	-55	Experimental	[30]

Table 4: Calculated variables of Ti_3Si and Ti_5Si_3 phases after optimization procedures. Vi1 in (J.(mol of atoms)$^{-1}$); Vi2 and Vi3 in (J.(mol of atoms)$^{-1}$).K^{-1}). The value for the reduced sum of squares was equal to 10 for both procedures. The values of the present investigation were compared with the values of the last assessment[11].

Description	Optimizing variables	Calculated values	Values of Seifert et al.[11]	Difference (%)
Gibbs energy for the formation of Ti_3Si_5	V11	-360707.460	-206191.45	75
	V12	15.4134911	16.4953	7
Gibbs energy for the formation of Ti_5Si_3	V21	-592931.498	-583564.31	2
	V22	3.78463760	2.68514	41
Gibbs energy for the formation of Ti_6Si_2	V31	-141301.038	417375.85	134
	V32	22.2273728	33.81017	34
Excess Gibbs energy (*:Ti,Si:Ti)	V41	47538.3043	43024.29	10
	V42	-4.64574985	-3.44194	35
Excess Gibbs energy (Si,Ti:*:Ti)	V51	-266180.152	-500000.0	47
	V52	27.3581605	40.0	31
Gibbs energy for the formation of Ti_3Si	V1	-186823.828	-500000.0	62
	V2	-92.5387205	0.79981	12600
	V3	11.6727301	-	-

Figure 3-a shows a general view of the calculated metastable Ti-Si phase diagram, indicating that the positions of the phase boundaries are in fair agreement with previous experimental results[2-4]. Figure 3-b shows a detail of the Ti-rich corner of the metastable Ti-Si phase diagram near the eutectoid reaction, Ti(β) → Ti(α) + Ti_5Si_3. The positions of the solvus lines and phase boundaries are in good agreement with previous experimental diagrams[2-4,6-7]. Figure 3-c compares the present assessment with the calculated Ti-Si phase diagram using COST 507 database[22]. The present assessment shows lower values for the Si solubility in the Ti(α) and Ti(β) phases, especially for the Ti(β) phase. Additionally, there is a significant difference in the inclination of the solvus line of the Ti(α) phase: in the present assessment there is a reduction of the Si solubility in the Ti (α) phase in lower temperatures, while in the version using COST 507 database there is an increase in the Si solubility in the Ti (α) phase in lower temperatures. The present assessment of the metastable Ti-Si phase diagram shows a better agreement with the experimental results[2-4,6-7] near the eutectoid region, Ti(β) → Ti(α) + Ti_5Si_3; and a more usual inclination of the Ti(α) solvus line when compared with the assessed phase diagram using the COST 507 database[22].

Figure 4-a compares the stable and metastable eutectoid reactions in the Ti-rich corner of the Ti-Si phase diagram obtained in the present investigation, indicating that the metastable diagram presents, as expected, an increase in the Si solubility in the Ti(α) and Ti(β) phases and a decrease in the eutectoid temperature. Additionally, the Ti_5Si_3 phase in equilibrium with Ti_3Si phase shows a slightly narrower range of Si solubility below the eutectic temperature, indicating higher Si solubility of the Ti_5Si_3 phase in equilibria with Ti(β) and Ti_3Si phases (see Figure 4-b).

It is worth mentioning that most experimental works on the Ti-Si and Ti-Si-X systems[1-5,12-20] did not perform chemical analysis of the samples after long isothermal heat-treatments to insure the lack of interstitial contamination. Some of these works, however, were careful enough to apply hardness measurements of control samples (before and after heat-treatments) to audit possible and critical interstitial contamination during the experimental work[1-4,6-7,12-14]. Some of the disagreements found in the literature about on the presence of the Ti_3Si in the Ti-Si and Ti-X-Si phase diagrams might be explained by the occurrence of interstitial contamination[1], as the presence of interstitials might promote the stability of the Ti_3Si phase [1,6-7,11]. In the classical work of Svechnikov et al.[5], for instance, they observed the presence of a Ti(β) + Ti_5Si_3 + Ti_3Si phases instead of Ti(β) +

Table 5: Experimental and calculated equilibrium for the "stable" and "metastable" Ti-Si phase diagrams. Deviations between experimental and calculated values above 5% were marked with (*).

Reaction	Parameter	Experimental	Calculated	Deviation (%)
$L \rightarrow Ti_5Si_3$	T (K)	2403	2441	1.6
	$X^{Si}(Ti_5Si_3)$	0.375	0.376	0.3
$L \rightarrow TiSi_2$	T (K)	1773	1757	0.9
	X^{Si} ($TiSi_2$)	0.667	0.667	0
$L \rightarrow \beta + Ti_5Si_3$	T (K)	1613	1638	1.6
	X^{Si} (L)	0.137	0.124	9.5*
	X^{Si} (β)	0.05	0.04	20*
	X^{Si} (Ti_5Si_3)	0.36	0.356	1.1
$L \rightarrow TiSi_2 + Si$	T (K)	1603	1604	0.1
	X^{Si} (L)	0.86	0.815	5.2*
	X^{Si} ($TiSi_2$)	0.667	0.667	0
	X^{Si} (Si)	1	1	0
$L \rightarrow TiSi_2 + TiSi$	T (K)	1743	1747	0.2
	X^{Si} (L)	0.641	0.637	0.6
	X^{Si} (TiSi)	0.5	0.5	0
	X^{Si} ($TiSi_2$)	0.667	0.667	0
$L + Ti_5Si_3 \rightarrow Ti_5Si_4$	T (K)	2193	2172	1.0
	X^{Si} (L)	0.48	0.503	4.8
	$X^{Si}(Ti_5Si_3)$	0.398	0.394	1.0
	$X^{Si}(Ti_5Si_4)$	0.444	0.444	0
$L + Ti_5Si_4 \rightarrow TiSi$	T (K)	1843	1843	0
	X^{Si} (L)	0.60	0.604	0.7
	X^{Si} (Ti_5Si_4)	0.444	0.444	0
	X^{Si} (TiSi)	0.5	0.5	0
$\beta + Ti_5Si_3 \rightarrow Ti_3Si$	T (K)	1443	1443	0
	X^{Si} (β)	0.04	0.028	30*
	X^{Si} (Ti_5Si_3)	0.36	0.359	0.3
	X^{Si} (Ti_3Si)	0.25	0.25	0
$\beta \rightarrow \alpha + Ti_3Si$	T (K)	1149	1143	0.5
	X^{Si} (β)	0.009	0.0088	2.2
	X^{Si} (α)	0.004	0.0037	7.5*
	$X^{Si}(Ti_5Si_3)$	0.25	0.25	0
$\beta \rightarrow \alpha + Ti_5Si_3$	T (K)	1130	1140	0.9
	X^{Si} (β)	0.011	0.0114	3.7
	X^{Si} (α)	0.005	0.0048	4.0
	$X^{Si}(Ti_5Si_3)$	0.375	0.3651	2.7

Table 6: Calculated values of the enthalpy (kJ/mol of atoms) and entropy (J/mol.K) of the formation of the intermetallic phases at 298 K – present work – compared with values of enthalpy found in the literature[11,20,25-30].

Phase	Average values of the enthalpy in the literature[11,25-30]	Ab-initio values of enthalpy[20]	Calculated values of enthalpy (kJ/mol of atoms)	Calculated values of entropy (J/mol.K)
Ti_3Si	-49.5	-47.11	-47.57	31.33
Ti_5Si_3	-73.9	-72.53	-74.12	25.78
Ti_5Si_4	-77.8	-74.63	-79.03	22.94
TiSi	-74.0	-72.23	-77.53	20.94
$TiSi_2$	-55.8	-49.87	-58.35	21.26

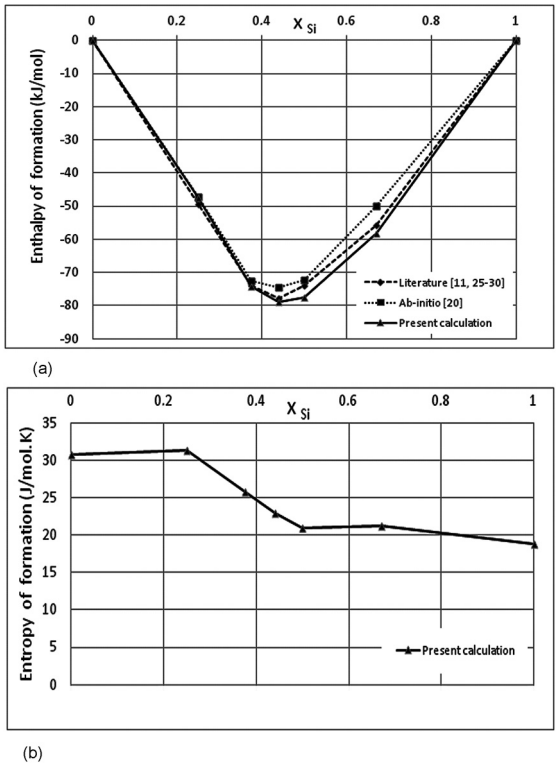

Figure 1: a) Enthalpies for the formation of the Si–Ti compounds, comparing the calculated results of the present work with the values found in the literature[11,20,25-30]; b) Entropies for the formation of the Si–Ti compounds.

Ti_5Si_3 phases after heat-treatment at 1493K for 120 h of Ti-Si alloys with Si contents below 25 at %Si, see Figure 2. This observation might suggest some interstitial contamination of the alloys during the experimental work of Svechnikov et al.[5]. Discrepancies were also observed in the investigation by Ramos et al.[16], which showed the presence of Ti_5Si_3 phase instead of Ti_3Si phase after isothermal heat-treatment for 90 hours at 1273K and 1373K of a Ti-25Si alloy, see Figure 2. Similarly, Costa et al.[17] showed the presence of Ti(α) + Ti_3Si phases instead of Ti(β) + Ti_3Si phases after isothermal treatment for 6 hours at 1273K of a Ti-13Si alloy, see Figure 2. These examples support previous suggestions made by Aaronson et al.[6,7] "that further experimental work in the Ti-rich corner of the Ti-Si system is needed" to explain experimental disparities, especially near the eutectoid region of the Ti-rich corner of the Ti-Si phase diagram; and that "some of these experimental discrepancies could explained by interstitial contamination".

More recently, Colinet and Tedenac[20] indicated by ab-initio calculations that the question of the stability of the Ti_3Si phase was in fact "controversial"; while Poletaev et al.[21] showed by ab-initio calculations that the Ti_5Si_3 phase was essentially more stable than the Ti_3Si phase at 0 K, adding a new light on the dispute over the stability of Ti_3Si phase in the Ti-Si and Ti-X-Si systems. In this sense, the present assessments aim to inspire further experimental work in the eutectoid region of the Ti-rich corner of the Ti-Si phase diagram in order to investigate the stability of Ti_3Si and Ti_5Si_3 phases; and the effect of interstitials on the stability of the Ti_3Si phase. The microstructural design of

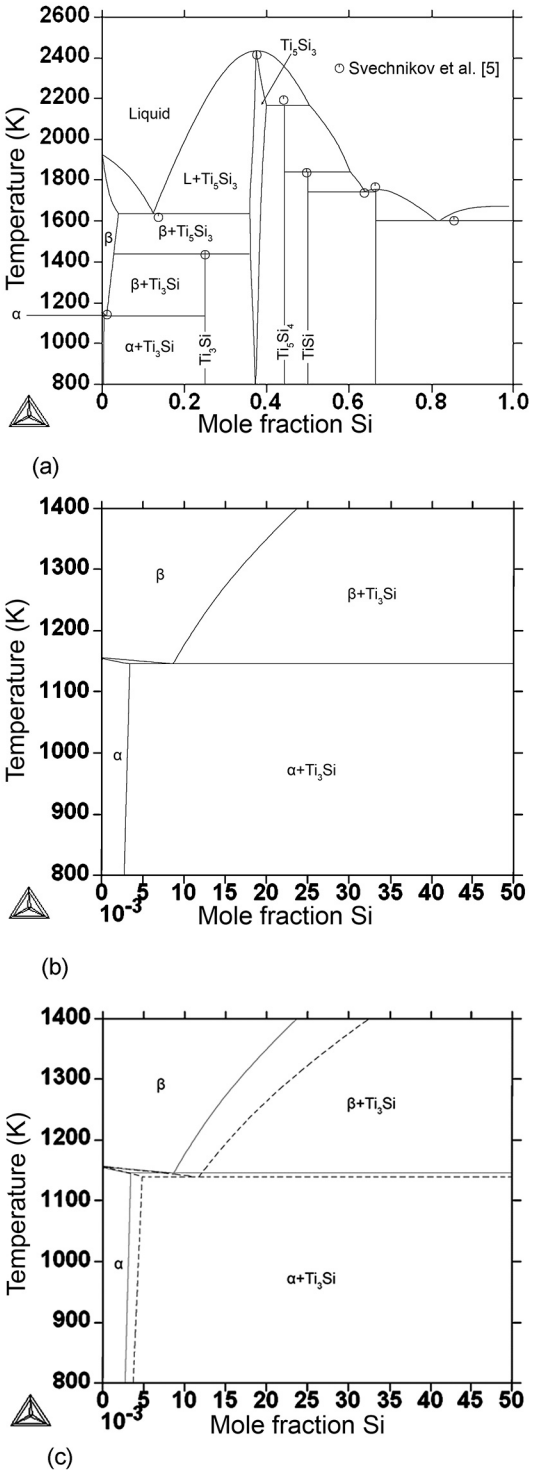

Figure 2: Assessed "stable" Ti-Si phase diagram. a) General view of the phase diagram, (β+Ti_5Si_3→Ti_3Si and β→α+Ti_3Si reactions); b) Detail of the eutectoid reaction, Ti(β) → Ti(α) + Ti_3Si, in the Ti-rich corner; c) Comparison between the present assessment and assessment (dotted lines) using COST 507 database[22].

commercial Ti-X-Si alloys requires the presence of enough Si in solid solution in the matrix to improve the oxidation resistance; and the precipitation of "strong" Ti-Si intermetallics, which

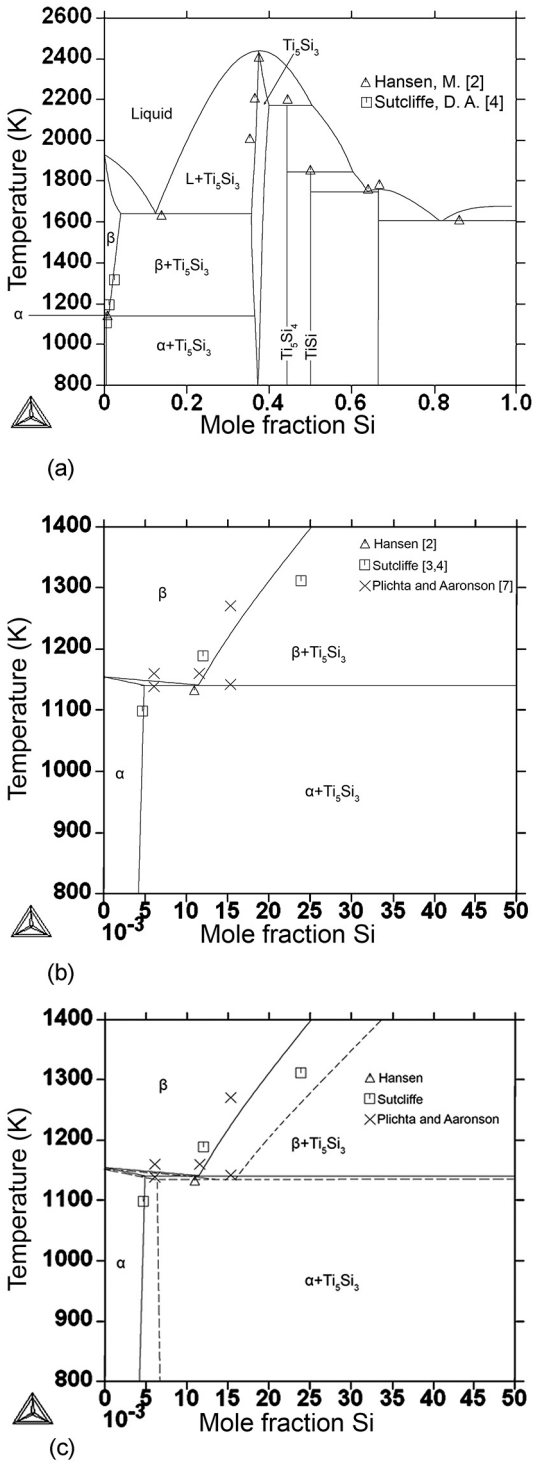

Figure 3: Assessed "metastable" Ti-Si phase diagram. a) General view of the Ti-Si phase diagram; b) Detail of the eutectoid reaction, $Ti(\beta) \rightarrow Ti(\alpha) + Ti_5Si_3$, in the Ti-rich corner; c) Comparison between the present assessment and assessment (dotted lines) using COST 507 database[22] with suspended Ti_3Si phase.

must be stable at service temperatures, to improve the creep resistance[1,21,32-36], so a better understanding of the Ti-rich corner of the Ti-Si phase diagram is needed.

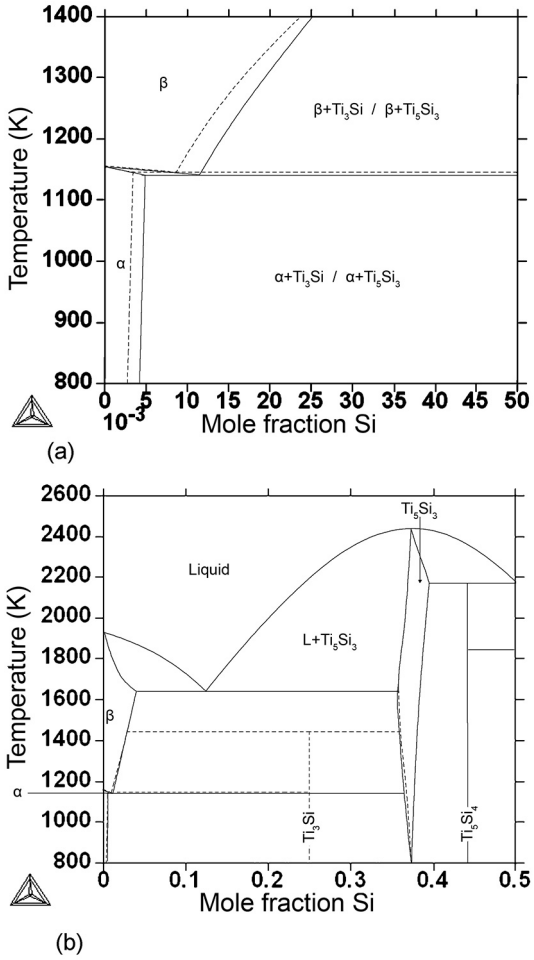

Figure 4: Comparison of the calculated stable (dotted lines) and metastable Ti-Si phase diagrams in the present investigation. a) Detail of the eutectoid reaction; b) Detail of the Si-solubility range of the Ti_5Si_3 phase.

4. Conclusions

Available experimental data allowed the calculation of the stable and metastable phase diagrams of the Ti-rich corner of the Ti-Si system.

The present assessment might be further improved by the use of a more complex description for the liquid phase and, more importantly, by the use of new experimental data near the eutectoid reaction of the Ti-rich corner of the Ti-Si phase diagram.

The present assessment of the "metastable" Ti-Si phase diagram showed a better agreement with the experimental results near the eutectoid region, $Ti(\beta) \rightarrow Ti(\alpha) + Ti_5Si_3$, and a more usual inclination of the $Ti(\alpha)$ solvus, when compared to the assessment using COST 507 database.

Further experimental work near the eutectoid region of the Ti-rich corner of the Ti-Si phase diagram is needed to solve the dispute over the stability of the Ti_3Si and Ti_5Si_3 phases.

5. Acknowledgments

The authors would like to thank the kind collaboration of Prof. V. Pastoukhov, Prof. C.G. Schöen, Prof. L.T.F Eleno and

Prof. S. Wolynec, all from Universidade de São Paulo, and Dr. A. H. Feller. This work is dedicated to the memories of Mr. A. C. Azevedo, Prof. H. M. Flower (Imperial College) and Mrs. B. F. Feller. The present investigation was funded by the Ministry of Education from Brazil (Coordination for the Improvement of Higher Education Personnel, CAPES) in a form of a MEng scholarship to Ms. M. Fiore.

6. References

1. Azevedo CRF. *Phase Diagram and Phase Transformations in Ti-Al-Si System* [PhD Thesis]. London: Imperial College, Department of Materials; 1996.
2. Hansen M, Anderko K. *Constitutions of binary alloys.* New York, Toronto, London: McGraw-Hill; 1958.
3. Sutcliffe DA. Alliage de titane et de silicium. *Revue de Metallurgie*. 1954;3:524-536.
4. Sutcliffe DA. Titanium-Silicon Alloys. *Metal Treatment and Drop Forging*. 1954;4:181-197.
5. Svechnikov VN, Kocherzhisky YA, Yupko LM, Kulik OG, Shinshkin EA. Phase Diagram of the Titanium-Silicon System. *Doklady Akademii Nauk SSSR*. 1970;193(2):393-396.
6. Plichta MR, Williams JC, Aaronson HI. On the existence of the $\beta \rightarrow \alpha_m$ transformation in the alloy systems Ti-Ag, Ti-Au, and Ti-Si. *Metallurgical and Materials Transactions A*. 1977;8(12):1885-1892.
7. Plitcha MR, Aaronson HI. The thermodynamic and kinetics of the $\beta \rightarrow a_m$ transformation in three Ti-X systems. *Acta Metallurgica.* 1978;26(8):1293-1305.
8. Kauffman L. Coupled phase diagrams and thermochemical data for transition metal binary systems-VI. *Calphad*. 1970;3(1):45-76.
9. Murray JL. *Phase diagrams of titanium binary alloys*. Novelty: ASM International:; 1987. p.289-293.
10. Vahlas C, Chevalier PY, Blanquet E. A Thermodynamic Evaluation of Four Si-M (M=Mo, Ta, Ti, W) Binary System. *Calphad*. 1989;13(3):273-292.
11. Seifert HJ, Lukas HL, Petzow G. Thermodynamic Optimization of the Ti-Si system. *Zeitschrift für Metallkunde*. 1996;87(1):2-13.
12. Azevedo CRF, Flower HM. Microstructure and phase relationships in Ti-Al-Si system. *Materials Science and Technology*. 1999;15(8):869-877.
13. Azevedo CRF, Flower HM. Experimental and calculated Ti-rich Corner of the Ti-Al-Si Ternary Phase Diagram. *Calphad*. 2002;26(3):353-373.
14. Azevedo CRF, Flower HM. Calculated ternary diagram of Ti-Al-Si system. *Materials Science and Technology.* 2000;16(4):372-381.
15. Bulanova M, Tretyachanko L, Golovkova M. Phase Equilibria in the Ti-rich corner of the Ti-Al-Si System. *Zeitschrift für Metallkunde*. 1997;88(3):256-265.
16. Ramos AS, Nunes CA, Coelho GC. On the peritectoid Ti_3Si formation in Ti-Si alloys. *Materials Characterization*. 2006;56:107-111.
17. Costa AMS, Lima GF, Rodrigues G, Nunes CA, Coelho GC, Suzuki PA. Evaluation of Ti_3Si phase stability from heat-treated rapidly solidified Ti-Si alloys. *Journal of Phase Equilibria and Diffusion*. 2010;31(1):22-27.
18. Li Z, Liao C, Liu Y, Wang X, Wu Y, Zhao M, et al. 700 ºC Isothermal Section of the Al-Ti-Si Ternary Phase Diagram. *Journal of Phase Equilibria and Diffusion*. 2014;35(5):564-574.
19. Kozlov AY, Pavlyuk VV. Investigation of the interaction between the components in the Ti -{Si, Ge}- Sb systems at 670 K. *Journal of Alloys and Compounds*. 2004;367(1-2):76-79.
20. Colinet C, Tedenac JC. Structural stability of intermetallic phases in the Si-Ti system. Point defects and chemical potentials in $D8_8$-Si_3Ti_5 phase. *Intermetallics*. 2010;18(8):1444-1454.
21. Poletaev DO, Lipnitskii AG, Kartamyshev AI, Aksyonov DA, Tkachev ES, Manokhin SS, et al. Ab initio-based prediction and TEM study of silicide precipitation in titanium. *Computational Materials Science*. 2014;95:456-463.
22. European Cooperation in the Field of Scientific and Technical Research, European Commission. COST 507 - Definition of thermochemical and thermophysical properties to provide a database for the development of new light alloys. Vol 1. Proceedings of the Final Workshop of COST 507, Vaals; 1997. Luxembourg: Office for Official Publications of the European Communities; 1998. Vol 2. Ansara I, Dinsdale AT, Rand MH, eds. Thermochemical Database for Light Metal Alloys Luxembourg: Office for Official Publications of the European Communities; 1998. Vol 3. Effenberg G, ed. Critical Evaluation of Ternary Systems. Luxembourg: Office for Official Publications of the European Communities; 1998.
23. Lukas HL, Fries SG, Sundman B. *Computational Thermodynamics: The Calphad Method*. Cambridge: Cambridge University Press; 2007.
24. Okamoto H. The C-Fe (carbon-iron) System. *Journal of Phase Equilibria*. 1992;13(5):543-565.
25. Robins DA, Jenskins I. The heats of formation of some transition metal silicides. *Acta Metallurgica*. 1955;3(6):598-604.
26. Topor L, Kleppa OJ. Standard enthalpies of formation of $TiSi_2$ and VSi_2 by high-temperature calorimetry. *Metallurgical and Materials Transactions A*. 1986;17(7):1217-1221.
27. Maslov VM, Neganov AS, Borovinskaya IP, Merzhanov AG. Self-propagating high-temperature synthesis as a method for determination of the heat of formation of refractory compounds. *Combustion, Explosion and Shock Waves*. 1978;14(6):759-767.
28. Kematick RJ, Myers CE. Thermodynamics of the Phase Formation of the Titanium Silicides. *Chemistry of Materials*. 1996;8(1):287-291.
29. Meschel SV, Kleppa OJ. Standard enthalpies of formation of some 3d transition metal silicides by high temperature direct synthesis calorimetry. *Journal of Alloys and Compounds*. 1998;267(1-2):128-135.
30. Coelho GC, David N, Gachon JC, Nunes CA, Fiorani JM, Vilasi M. *Entalpias de formação de fases intermetálicas dos sistemas Ti–Si, Ti–B e Ti–Si–B medidas por calorimetria de síntese direta*. In: Associação Brasileira de Metalurgia e Materiais. Anais do 61° congresso Anual da ABM. Rio de Janeiro, Brasil. São Paulo: ABM; 2006. p. 1300-1308.
31. Thermo-Calc Data optimization User Guide, Version 2015a. *Foundation of Computational Thermodynamics Stockholm, Sweden*. [Accessed: 2015 Nov 15]. Available from: http://www.thermocalc.com/media/30890/Data-Optimisation-User-Guide-for-Thermo-Calc.pdf
32. Frommeyer G, Rosenkranz R, Lüdecke C. Microstructure and properties of the refractory intermetallic Ti_5Si_3 compound and the unidirectionally solidified eutectic Ti-Ti_5Si_3 alloy. *Zeitschrift für Metallkunde*. 1990;81:307-313.
33. Zhang L, Wu J. Ti_5Si_3-based alloys: alloying behavior, microstructure and mechanical property evaluation. *Acta Materialia*. 1998;46(10):3535-3546.
34. Kishida K, Fujiwara M, Adachi H, Tanaka K, Inui H. Plastic deformation of single crystals of Ti_5Si_3 with the hexagonal $D8_8$ structure. *Acta Materialia*. 2010;58(3):846-857.
35. Williams JJ. *Structure and high-temperature properties of Ti5Si3 with interstitial additions* [PhD Thesis]. Iowa: Iowa State University; 1999.
36. Kastenhuber M, Rashkova B, Clemens H, Mayer S. Enhancement of creep properties and microstructural stability of intermetallic β-solidifying γ-TiAl based alloys. *Intermetallics*. 2015;63:19-26.

Annex 1: Thermodynamic description of the phases of the Ti-Si system

LIQUID
EXCESS MODEL IS REDLICH-KISTER_MUGGIANU
CONSTITUENTS: SI,TI
G(LIQUID,SI;0)-H298(DIAMOND_A4,SI;0) =
298.15<T< 1687.00: +50696.4-30.0994*T+2.09307E-21*T**7+GHSERSI
1687.00<T< 6000.00: +49828.2-29.5591*T+4.20369E+30*T**(-9)+GHSERSI
G(LIQUID,TI;0)-H298(HCP_A3,TI;0) =
298.15<T< 1300.00: +12194.415-6.980938*T+GHSERTI
1300.00<T< 1941.00: +368610.36-2620.99904*T+357.005867*T*LN(T)-.155262855*T**2+1.2254402E-05*T**3-65556856*T**(-1)+GHSERTI
1941.00<T< 6000.00: +104639.72-340.070171*T+40.9282461*T*LN(T)-.008204849*T**2+3.04747E-07*T**3-36699805*T**(-1)+GHSERTI
L(LIQUID,SI,TI;0) = -255852.17+21.87411*T
L(LIQUID,SI,TI;1) = +25025.35-2.00203*T
L(LIQUID,SI,TI;2) = +83940.65-6.71526*T
BCC_A2
EXCESS MODEL IS REDLICH-KISTER_MUGGIANU
2 SUBLATTICES, SITES 1: 3
CONSTITUENTS: SI,TI: VA
G(BCC_A2,SI:VA;0)-H298(DIAMOND_A4,SI;0) = +47000-22.5*T+GHSERSI
G(BCC_A2,TI:VA;0)-H298(HCP_A3,TI;0) =
298.15<T< 1155.00: -1272.064+134.71418*T-25.5768*T*LN(T)
-6.63845E-04*T**2-2.78803E-07*T**3+7208*T**(-1)
1155.00<T< 1941.00: +6667.385+105.366379*T-22.3771*T*LN(T)+
.00121707*T**2-8.4534E-07*T**3-2002750*T**(-1)
1941.00<T< 4000.00: +26483.26-182.426471*T+19.0900905*T*LN(T)
-.02200832*T**2+1.228863E-06*T**3+1400501*T**(-1)
L(BCC_A2,SI,TI:VA;0) = -275629.1+42.5094*T
L(BCC_A2,SI,TI:VA;1) = +25025.35-2.00203*T
L(BCC_A2,SI,TI:VA;2) = +83940.65-6.71526*T
DIAMOND_A4
EXCESS MODEL IS REDLICH-KISTER_MUGGIANU
CONSTITUENTS: SI,TI
G(DIAMOND_A4,SI;0)-H298(DIAMOND_A4,SI;0) = +GHSERSI
G(DIAMOND_A4,TI;0)-H298(HCP_A3,TI;0) = +25000+GHSERTI
L(DIAMOND_A4,SI,TI;0) = +80*T
HCP_A3
EXCESS MODEL IS REDLICH-KISTER_MUGGIANU
2 SUBLATTICES, SITES 1: .5
CONSTITUENTS: SI,TI : VA
G(HCP_A3,SI:VA;0)-H298(DIAMOND_A4,SI;0) = +49200-20.8*T+GHSERSI
G(HCP_A3,TI:VA;0)-H298(HCP_A3,TI;0) = +GHSERTI
L(HCP_A3,SI,TI:VA;0) = -302731.04+69.08469*T
L(HCP_A3,SI,TI:VA;1) = +25025.35-2.00203*T
L(HCP_A3,SI,TI:VA;2) = +83940.65-6.71526*T
SI2TI
2 SUBLATTICES, SITES 2: 1
CONSTITUENTS: SI: TI
G(SI2TI,SI:TI;0)-2*H298(DIAMOND_A4,SI;0)-H298(HCP_A3,TI;0) =
-175038.5+4.548*T+GHSERTI+2*GHSERSI

Continued Annex 1

SI4TI5
2 SUBLATTICES, SITES 4: 5 CONSTITUENTS: SI : TI G(SI4TI5,SI:TI;0)-4*H298(DIAMOND_A4,SI;0)-5*H298(HCP_A3,TI;0) = -711000+22.37355*T+4*GHSERSI+5*GHSERTI
SITI
2 SUBLATTICES, SITES 1: 1 CONSTITUENTS: SI : TI G(SITI,SI:TI;0)-H298(DIAMOND_A4,SI;0)-H298(HCP_A3,TI;0) = -155061.7 +7.6345*T+GHSERSI+GHSERTI
SITI3
2 SUBLATTICES, SITES 1: 3 CONSTITUENTS: SI : TI G(SITI3,SI:TI;0)-H298(DIAMOND_A4,SI;0)-3*H298(HCP_A3,TI;0) = +**V1**+**V2***T +**V3***T*LN(T) +GHSERSI+3*GHSERTI
SI3TI5
EXCESS MODEL IS REDLICH-KISTER_MUGGIANU 3 SUBLATTICES, SITES 2: 3: 3 CONSTITUENTS: SI,TI : SI,TI: TI G(SI3TI5,SI:SI:TI;0)- 5*H298(DIAMOND_A4,SI;0)-3*H298(HCP_A3,TI;0) = +**V11**+**V12***T+5*GHSERSI+3*GHSERTI G(SI3TI5,TI:SI:TI;0)-3*H298(DIAMOND_A4,SI;0)-5*H298(HCP_A3,TI;0) = +**V21**+**V22***T+5*GHSERTI+3*GHSERSI G(SI3TI5,SI:TI:TI;0)-2*H298(DIAMOND_A4,SI;0)-6*H298(HCP_A3,TI;0) = +**V31**+**V32***T+2*GHSERSI+6*GHSERTI G(SI3TI5,TI:TI:TI;0)-8*H298(HCP_A3,TI;0) = +40000+20*T+8*GHSERTI L(SI3TI5,SI:SI,TI:TI;0) = +**V41**+**V42***T L(SI3TI5,TI:SI,TI:TI;0) = +**V41**+**V42***T L(SI3TI5,SI,TI:SI:TI;0) = +**V51**+**V52***T L(SI3TI5,SI,TI:TI:TI;0) = +**V51**+**V52***T